Multiscale Curvature Estimation for Segmenting a Triangle Mesh into Shape Features

M. Mortara† G. Patané†

†Istituto di Matematica Applicata e Tecnologie Informatiche,
Consiglio Nazionale delle Ricerche, Genova, Italy.
e-mail:{michela,patane}@ge.imati.cnr.it, **web:** http://www.ge.imati.cnr.it

Abstract

Tools for the automatic decomposition of a surface into shape features facilitate the editing, matching, texturing, morphing, compression, and simplification of 3D shapes. Different features, such as flats, limbs, tips, pits, and various blending shapes may be characterized in terms of local curvature and differential properties of the surface. Because Gaussian curvature is extremely sensitive to small perturbations in the surface smoothness and to quantization effects when evaluated on triangulated surfaces, we propose a multi-resolution approach, which not only estimates the curvature of a vertex over neighborhoods of variable size, but also takes into account the topology of the surface in that neighborhood. We describe an efficient approach for computing these characteristics at different scales and for using them to identify features, based on easily formulated filters, that may capture the needs of a particular application.

Categories and Subject Descriptors (according to ACM CCS): I.3.3 [Computer Graphics]: multiscale analysis, shape feature extraction, triangle-mesh decomposition.

1. Introduction

Shape analysis and coding is a challenging problem in Computer Vision and Graphics. An ideal shape description should be able to capture and compute the main features of a given shape and organize them into an abstract representation which can be used to automate processes such as matching, retrieval or comparison of shapes. We have tackled the problem in the context of 3D objects represented by triangular meshes, having in mind that a good shape description should be able to distinguish between global and local features and should be based on geometric properties of the shape which are invariant under rotation, translation and scaling [3]. To characterize a shape we have used the paradigm of *growing bubbles*[9]: a set of spheres of increasing radius R_i, $i = 1,\ldots,n$ is drawn, whose centers are at each vertex of the mesh, and whose radius represents the scale at which the shape is analyzed. The number of intersections between the spheres and the shape boundary gives a first qualitative characterization of the shape in a 3D neighborhood of each vertex. Then, a number of metric and geometric parameters are computed to refine the classification and detect specific features such as sharp protrusions and well, mounts or dips, blends and branching parts.
The resulting description provides an insight on the presence of features together with their morphological type, persistence at scale variation, amplitude and/or size. The decomposition is algorithmically simple, independent on the orientation of the object in space and equally distributed in all directions. The multi-scale approach and the chosen descriptors define a view-independent decomposition and reduce the influence of noise on the shape classification.
In this paper we focus on the method adopted for the segmentation, and possible applications of the results are proposed in [8, 11], where a skeleton describing a shape from the point of view of its sharpest protrusions, and the axis computation of tubular parts are presented.

The paper is organized as follows: in Section 2 previous work and basic concepts on differential geometry are summarized. The approach to shape decomposition is detailed

in Section 3; finally, results and applications are described in the last section.

2. Discrete curvature estimation

Given a surface Σ, the Gaussian curvature represents a measurement at any point $p \in \Sigma$ which is the excess per unit area of a small patch of the surface, i.e., how "curved" it is. The definition of the curvature at each point of a triangulation is not trivial because a triangular mesh is a piecewise continuous function whose second derivatives are, almost everywhere, zero. More precisely, the curvature on a triangulation is concentrated along edges and at vertices, since every other point has a neighborhood homeomorphic to a planar Euclidean domain whose Gaussian curvature is null.

The methods proposed in the literature for curvature evaluation can be classified into two main groups: *continuous-based* and *property-based* algorithms.
The first ones are developed transforming the discrete case to the continuous one by using a local fitting of the surface which enables to apply standard definitions. For example, in [6] an approximation is derived at each vertex by applying the continuous definition to a least-square paraboloid fitting its neighboring vertices, while in [12] it is evaluated by estimating its tensor curvature.
The algorithms of the second group start from basic properties of continuous operators but directly applied to the discrete settings. The methods proposed in [1, 10] are based on the Laplace-Beltrami operator and the Gauss map, thus guaranteeing the validity of differential properties such as area minimization and mean curvature flow [5].
Previous approaches are usually sensitive to noise and small ondulations, requiring smoothness conditions on the input mesh or a multi-resolution simplification aimed at discarding local details and artifacts. Furthermore, the smoothing process used to get stable and uniform curvature estimations introduces a deficiency in the magnitude evaluation and, consequently, difficulties in the accurate distinction between planar patches and curved surfaces with low curvature.

Our framework is based on the use of the angle excess, computed in the discrete domain represented by triangular meshes. As presented also in [2, 10], the angle excess nicely evaluates the Gaussian curvature at mesh vertices. Given a closed curve γ on a surface Σ, let us indicate with T_γ the total turning that the unit tangent t undergoes when it is carried along γ, defined as the sum of the local turnings, i.e. *exterior angles* [7]. Then the quantity $I_\gamma = 2\pi - T_\gamma$ is called the *angle excess* of the curve γ and it is related to the curvature of Σ within γ, as described by the Gauss-Bonnet formula.

Gauss-Bonnet Formula
Let γ be a curvilinear polygon of class C^2 on a surface patch of class C^k, $k \geq 3$. Suppose γ has a positive orientation and its interior on the patch is simple connected. Then

$$\int_\gamma \kappa_g ds + \iint_\Omega K dS = 2\pi - \sum_i \alpha_i = I_\gamma \qquad (1)$$

where κ_g is the geodesic curvature along γ, Ω is the union of γ and its interior, K is the Gaussian curvature and α_i the exterior angles of γ.

For instance, let us consider the region $Star(p)$ on the surface defined by the triangles incident to a vertex p. The boundary of $Star(p)$ defines a closed path on the mesh, to which we may apply the Gauss-Bonnet formula (1). Since the geodesic curvature along the boundary is zero (edges are straight), the total curvature at p is simply quantified by the sum of the exterior angles. Roughly speaking, we can imagine to locally cut $Star(p)$ along any of the edges incident in p, and to develop the $Star(p)$ onto the plane without shrinking the surface. The sum of the exterior angles corresponds to the sum of the angles at p in the $Star(p)$. This result is consistent with the intrinsic nature of the Gaussian curvature since the angle excess only depends on the angles, that is, this value does not change if the mesh is deformed preserving the distance between points. Also, the computation of angle excess can be performed without resorting to any coordinate system, as the angles may be obtained using only the edge length and not the vertex coordinates.

3. Decomposition of triangular meshes

Our approach for describing a 3D shape integrates boundary and information on the interior volume of the shape. The link between closed paths on the input surface and curvature has suggested us to specialize its study to the family of curves built by intersecting the surface with spheres centered in each of its points.

Given a 3D mesh Σ and a set of radii $R_i, i = 1..n$, let us call $S(p,R_i)$ the sphere of radius R_i and center p, and $\gamma(p,R_i)$ the boundary of the region of Σ containing p delimited by the intersection curves between the mesh and $S(p,R_i)$. Other regions of intersection might occur, but only the one containing p is taken into account. The first morphological characterization of the surface at vertex p at scale R_i is given by the number of connected components of $\gamma(p,R_i)$. We consider the following cases:

- 1 *component*: the surface around p can be considered topologically equivalent to a plane (see Figure 1(a)),
- 2 *components*: the surface around p is tubular-shaped (see Figure 1(b)),
- $n \geq 3$ *components*: in a neighborhood of p a branching of the surface occurs (see Figure 1(c)).

In topological terms, two components identify a handle in the object, three or more components locate a split. If $\gamma(p,R_i)$ is made by only one component, the angles excess is computed and the vertex is classified as sharp, rounded or

blend. If $\gamma(p,R_i)$ is made by two components, their lengths are used to distinguish among tubular and cylindrical shapes. For branching parts, no further geometric parameters are computed (see Table 1).

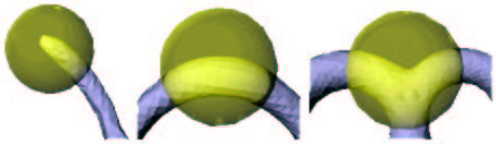

(a) (b) (c)

Figure 1: *Evaluation of the number of the connected components.*

With reference to the properties of the obtained intersection curve $\gamma(p,R_i)$ at scale R_i, p is classified according to the number of its connected components, curvature if $\gamma(p,R_i)$ has only one component, relative length if $\gamma(p,R_i)$ has two components, and a concavity/convexity check in all cases. These classification criteria will be treated separately in the following sections. The combination of all these steps leads to a complete characterization of vertices, which expresses both the geometric and morphological properties of the surface.

3.1. Curvature characterization

As described above, when $\gamma(p,R)$ has only one boundary component, the curvature at a point p, at scale R, is approximated by the angle excess of $\gamma(p,R)$. Instead of using the angle excess, we use the length of $\gamma(p,R)$ divided by the radius R, $L_{\gamma(p,R)} = L/R$. Note that this value has the dimension of an angle and it always assumes a positive value. Since we want to characterize the curvature of a surface, vertices will be labeled as a sharp, rounded, or blend points according to their approximate curvature values by establishing some thresholds on the interval $[0,+\infty)$. The choice of these thresholds does not represent a lack of generality, since they are tuned on the evaluated values on sampled surfaces. We can distinguish the following cases:

- *sharp vertices*: let us consider a cone surface with p a spike point and $\alpha \in (0,\pi/2]$ the half amplitude of the cone. Intersecting the cone with a sphere centered in p and with radius R generates a circular curve of length $(2\pi R)\sin(\alpha)$ where $L_{\gamma(p,R)} = (2\pi)\sin(\alpha)$ is an increasing function of $\alpha \in (0,\pi/2]$: the less is α, the more "pointy" is the surface around p. We consider p a sharp vertex if $\alpha \leq \pi/4$ and consequently the curvature threshold is set to $T_s = \sqrt{2}\pi$; anyway, the option of changing the threshold is available to the user who can tune the α value for each input surface.
- *rounded/blend*: to distinguish between these two situations we observe that the surface is rounded in a neighborhood of a point if its curvature continuously decreases, becomes at first "flat" and then "blend". Now consider the intersection between the sphere and a plane; in this trivial case the length of the intersection curve is equal to $2\pi R$ and $L_{\gamma(p,R)} = 2\pi$; it follows that the threshold which discriminates between "rounded" and "blend" is set to $T_b = 2\pi$.

Summarizing, the characterization of a point p at scale R is set as follows:

- $0 \leq L_\gamma(p,R) \leq \sqrt{2}\pi$: p is "sharp",
- $\sqrt{2}\pi < L_\gamma(p,R) \leq 2\pi$: p is "rounded",
- $L_\gamma(p,R) > 2\pi$: p is "blend".

The different cases are shown in Figure 2.

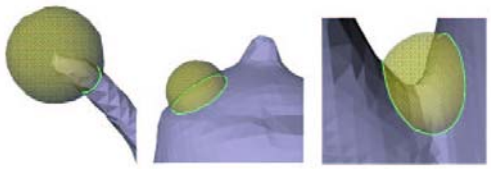

(a) (b) (c)

Figure 2: *(a) Sharp vertex, (b) rounded vertex, (c) blend vertex.*

3.2. Relative length characterization

Now we consider the case of two connected components in the intersection curve $\gamma(p,R)$. As mentioned above, this means that p lies on a region of the surface having an elongated shape, like a tubular protrusion or a handle around a hole in the object. We can specialize this remark as follows: if the length of the two intersection components is nearly the same, the shape at scale R can be approximately considered cylindrical; if one is much longer than the other, it means that the shape may be seen as a cone (see Figure 3). Let γ_1 and γ_2 be the two intersection components, and l_1, l_2 their lengths with $l_1 \geq l_2$. The shape is considered conical if $l_1 \geq 2l_2$. The related threshold is $T_c = 1/2$, thus guaranteeing that the amount l_2/l_1 (belonging to $[0,1]$) uniquely determines whether the local shape of the surface around p is cylindrical or conic.

3.3. Status characterization

The extraction of morphological features on a surface is based on different operators each of them provides a specific, e.g. geometric, topological, approach to its description. For instance, in the case of one connected components in $\gamma(p,R)$, to discriminate between convex and concave vertices would lead to classify a "sharp" point as a peak or a pit, a "rounded" point as a mount or a dip; the distinction of convex/concave does not make sense for "blend" points. An analogous to the convexity/concavity property can be defined for vertices with two or more connected components in

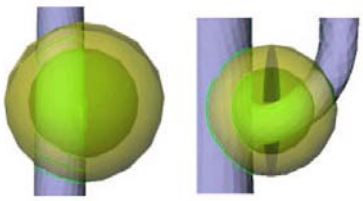

(a) (b)

Figure 3: *Example of conical (a), and cylindrical (b) parts of a triangular mesh.*

$\gamma(p,R)$, a criterion for distinguishing a handle from a deep tubular depression of the object.

Let us consider the case of one component first. As for curvature computation, concavity/convexity evaluation at a vertex p of a triangular mesh is strongly affected by noise and depends on the local topology of the $Star(p)$; furthermore, point coordinates can be slightly affected by noise resulting in a complete different classification. For these reasons, the method adopted for assessing a "convex" or "concave" label to a vertex p at scale R again uses the intersection of the mesh with the sphere. In the case of one connected component of the intersection curve, the center of mass b of γ and the average normal N of intersected triangles are computed. The vertex p is considered concave (resp. convex) at scale R, if p lies "below" (resp. "above") γ, that is $N \bullet (b - p) > 0$ (resp. < 0).

When $\gamma(p,R)$ has two or more intersection components, we can distinguish between the case in which the local shape is full or empty (i.e. the patch of surface inside the sphere encloses a volume or not), in analogy with the property of convex/concave mentioned above for points generating one intersection curve. This statement discriminates between a tubular protrusion and a tubular depression of the surface when the intersection components are two; between a branch on the outer surface or a splitting cavity for three or more connected components.

3.4. Mesh decomposition

The focus of this section is the integration of the different characterizations to achieve a segmentation of the input mesh into morphological features. In Table 1, a summary of the labels assigned to vertices for each scale is given, and in Figure 4 some examples of the label assessments are shown.

Given a set of radii $R_i, i = 1..n$, a n-dimensional vector of morphological labels (i.e. feature types at the corresponding scales) is assigned to each vertex of the mesh. Shape features of the mesh are then identified by connected regions of vertices with the same label at a given scale, and the geometric parameters computed to assign the label characterize the feature from a metric point of view. These parameters, together with the persistence of type through the scale values, can be used to distinguish global and local features with respect to the scale range.

Table 1: *Morphological feature characterization.*

Shape	Color	Inters.	Ratio	Status
Peak	Red	1	$L/R \leq T_p$	Convex
Pit	Blue	1	$L/R \leq T_p$	Concave
Mount	Orange	1	$T_p < L/R \leq T_b$	Convex
Dip	Cyan	1	$T_p < L/R \leq T_b$	Concave
Blend	Pink	1	$L/R > T_b$	–
Limb	Yellow	2	$L_2/L_1 \geq T_c$	Full
Well	Violet	2	$L_2/L_1 \geq T_c$	Empty
Joint	Brown	2	$L_2/L_1 < T_c$	Full
Funnel	Dark	2	$L_2/L_1 < T_c$	Empty
Split	Green	3 or more	–	Full
HollowY		3 or more	–	Empty

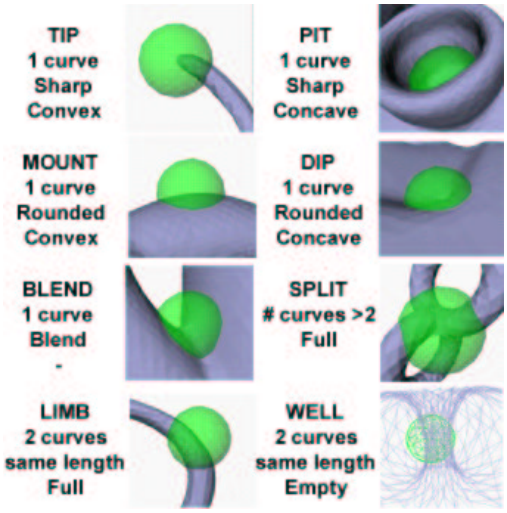

Figure 4: *Examples of label assessment.*

Selecting the scale of interest, the surface can be rendered using a color-coding of the feature labels. The achieved decomposition is an affine-invariant segmentation of disjoint, non-empty subsets which code the geometry and shape evolution through scale changes. In Figure 5(a) a first example of the resulting decomposition is shown, with a set of ten radii. The different views show the results with eight different radii, and the colors are those related to Table 1.

It is interesting to notice the good stability of the segmentation with respect to noise as shown in Figure 6: peak and limb regions are well preserved.

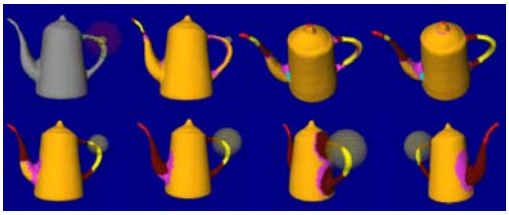

(a)

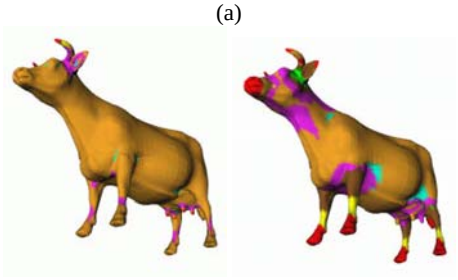

(b)

Figure 5: *(a) Shape segmentation on the pot (8 radii) and (b) on the cow model (2 radii).*

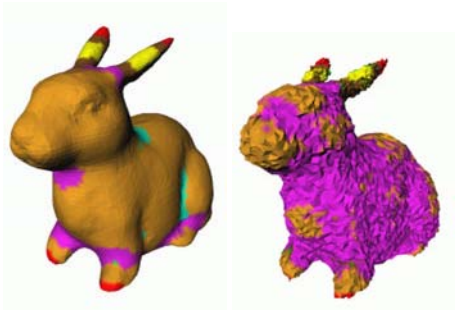

(a) (b)

Figure 6: *Shape segmentation (a) on the rabbit, and (b) on the same model with added noise.*

As discussed in the previous sections, curvature-based segmentation algorithms usually involve local measures and therefore are affected by noise. With our framework, the curvature is analyzed in a neighborhood whose size depends on R: for small values of R, such as the average length of the edges incident in p, the curvature approximation resembles the discrete curvature estimation proposed in [1] and suffers of the same problems while, for increasing values, it becomes more stable to noise. On the other hand, a too large radius can give a meaningless result. In the same way, small radii can be used to determine detail features while bigger ones are able to capture global characteristics of the surface. From these considerations, it follows that the choice of R is related to the scale of the features which have to be extracted, and the use of a set of increasing radii is suitable for performing a multi-scale analysis of the shape.

3.5. Results and discussion

The defined tools allow us to analyze a shape at different scales, and to derive information about the persistence of a shape feature across the scale range.

It is possible to define a coarse feature-based query language, which allows the user to submit a query like "which are the vertices whose feature type is PEAK at scale 3 and MOUNT at scale 6?", simply by means of a query vector with wild cards, and the AND Boolean operator(for instance, (*,*,P,*,*,M,*,*,*,*) would specify the above query.). In the example shown in Figure 5 (b), some details labeled as PEAK (depicted in red) at the smaller scale are lost at the higher one. By querying all PEAK vertices at at least one scale it is possible to obtain the union of all the PEAK regions through the scales (see Figure 7).

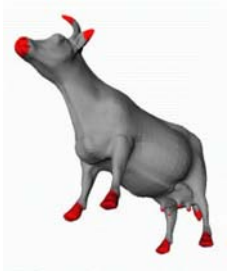

Figure 7: *Red areas are the union of vertices labelled as PEAK at at least one scale.*

Using the described language, the mesh can be analyzed in a rather flexible way. Two possible applications of these shape feature extraction at different scales are detailed in the following: protrusion-based skeleton extraction and axis computation of tubular parts, also described in [8, 11]. The first application consists of identifying PEAK regions at the chosen scale (or at several scales) and then, starting from the center of these regions, propagating in parallel pseudo-geodesic circles on the surface until the whole model is covered. Joining the barycenters of the adjacent pseudo-geodesic circles results in a skeleton of the shape whose terminal nodes are the tip of the selected protrusions (see Figure 8(a)). On the other hand, we may be interested in tubular parts, which include both long protrusions and thin handles of the object: then, the LIMB regions are selected and a medial loop of edges surrounding the tube is computed. Starting from the barycenter of the medial loop, the intersection curves between the mesh and the sphere centered in the barycenter are calculated. Then, the center of the sphere is joined with the two barycenters of the computed intersection curves, and the process is repeated until the length of the intersection curves varies too much. The line joining the barycenters of all the intersection curves gives the tube axis (see Figure 8(b)). The result of both algorithms on the same pot model are finally shown in Figure 9.

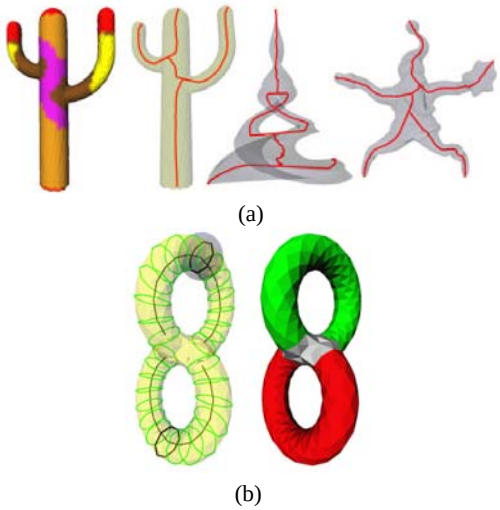

(a) (b)

Figure 8: *(a) Examples of protrusion-based skeleton extraction, (b) example of tube recognition and axis computation.*

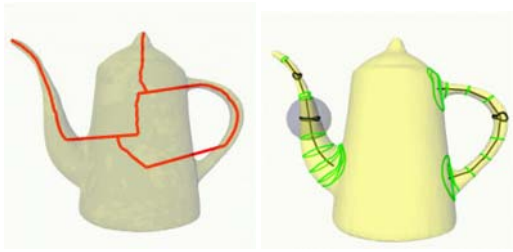

(a) (b)

Figure 9: *(a) Protrusion-based skeleton extraction, (b) tube recognition and axis computation performed on the same model.*

Acknowledgements

This work has been partially supported by the National Project "MACROGeo: Metodi Algoritmici e Computazionali per la Rappresentazione di Oggetti Geometrici", FIRB grant. The authors would like to thank Jarek Rossignac (Georgia Institute of Technology) and all the people of the Shape Modelling Group at IMATI-CNR, in particular Bianca Falcidieno and Michela Spagnuolo for their useful suggestions.

References

1. M. Desbrun, M. Meyer, P. Schroeder, A.H. Barr, "Discrete Differential-Geometry Operators in *n*D", July 22, 2000. URL: http://www.multires.caltech.edu/pubs/pubs.htm
2. Falcidieno, B., Spagnuolo, M.: Geometric Reasoning for the Extraction of Surface Shape Properties. *Communicating with the Virtual World*, N.Magnenat Thalmann and D. Thalmann (Eds.), Springer-Verlag, (1993)
3. Falcidieno, B., Spagnuolo, M.: A Shape-abstraction paradigm for modelling geometry and semantics. *Proceedings of Computer Graphics International 1998*, IEEE Computer Society Press (1998)
4. Gonzales, R.C., Woods, R.E.: *Digital Image Processing*. Reading, MASS.: Addison-Weshley, 1992.
5. V. Guillemin, and A. Pollack: *Differential Topology*, Englewood Cliffs, NJ: Prentice-Hall, 1974.
6. B. Hamman: Curvature Approximation for Triangulated Surfaces, *Computing Suppl.* 8, 1993, pp. 139-153.
7. Lipschutz, M.M.: *Theory and Problems of Differential Geometry*. Schaum's Outline Series.
8. Mortara, M., Patané, G.: Shape-Covering for Skeleton Extraction. In *International Journal on Shape Modeling*, Vol. 8, Num. 2, pp. 139-158.
9. Mortara M., Patanè G., Spagnuolo M., Falcidieno B., Rossignac, J.: *Blowing Bubbles for the Multi-scale Analysis and Decomposition of Triangle Meshes*. To appear in Algorithmica, Special Issues on Shape Algorithms, 2003.
10. Polthier, K., Scmies, M.: Straighhtest Geodesic polhedral Surfaces. In H.C. Hege and K. Polthier, editors, *Mathematical Visualization*. Springer Verlag, 1998.
11. Mortara, M., Patané, G., Falcidieno, B., Spagnuolo, M., Rossignac, J.: Plumber, the tube finder. *Technical Report n. 1/2003*, CNR-IMATI, Genova.
12. Taubin, G.: Estimating the Tensor Curvature of a Surface from a Polyhedral Approximation, *Fifth International Conference on Computer Vision (ICCV'95)*.